Coulomb breakup of one-neutron halo nuclei

M. Zadro*

Rudjer Bošković Institute, P.O. Box 180, HR-10002 Zagreb, Croatia
(Received 27 June 2004; published 8 October 2004)

The Coulomb breakup of one-neutron halo nuclei is studied within the postform distorted-wave Born approximation (DWBA) theory. A method of evaluation of the DWBA breakup amplitude in momentum space is presented. The theory is applied to the Coulomb breakup of the ^{11}Be and ^{19}C halo nuclei on ^{208}Pb at the beam energy of ~ 70 MeV/nucleon. Calculations for relative energy spectra are compared with available experimental data. Good agreement in shape is found for low relative energies. Comparison with the results obtained using a local momentum approximation to the DWBA amplitude shows that the effects of this additional approximation are substantial. The DWBA calculations are also compared to those of an adiabatic breakup theory. The two theories lead to significantly different results.

I. INTRODUCTION

The investigation of neutron halo nuclei has attracted significant interest in the past decades. In a simplified picture these nuclei are described as a well-defined core surrounded by a diffuse halo with a valence neutron(s) [1–3]. Breakup reactions, in which the valence neutron is removed from the halo nucleus, are used to study the properties of the halo structure. Coulomb breakup is an important reaction channel in the scattering of halo nuclei from highly charged targets. Because of the simplicity of the reaction mechanism, the Coulomb breakup could be a very important source of information about the structure of neutron halo nuclei. However, in order to extract reliable structure information from experimental data, the adequacy of the reaction formalism must be ascertained.

There are a number of different theoretical approaches to the study of the Coulomb breakup of neutron halo nuclei (see, e.g., Ref. [4] for a recent review). In some of these approaches the Coulomb and nuclear breakups are treated at the same time—e.g., Refs. [5–9]. Most of the methods are based on a semiclassical approximation: the relative motion between the projectile and target is treated classically. The experimental data are usually analyzed within the framework of first-order perturbation theory [10–16]. The main semiclassical methods which include higher-order effects are explicit inclusion of higher-order terms [17,18], coupled channel calculations [19,20], and direct numerical solution of the time-dependent Schrödinger equation [5,6,9,21–26].

The Coulomb breakup has also been investigated within fully quantum mechanical approaches. The post-form distorted-wave Born approximation (DWBA) was used earlier to study the breakup of light stable nuclei [27]. Later, this theory was also applied to the Coulomb breakup of neutron halo nuclei—e.g., Refs. [28,29]. The theory is first order in the interaction between the core and valence particle; it assumes that the excitation of the projectile is weak. Recently, a theory of Coulomb breakup has been formulated within the framework of an adiabatic model [30–32]. The model assumes that the excitation energy of the projectile is small compared with the energy of the projectile-target relative motion. This assumption leads to a simple bremsstrahlung expression for the breakup amplitude. In both the adiabatic and DWBA approaches the Coulomb interaction between the core and target is taken into account to all orders.

In applications of the DWBA theory to the Coulomb breakup of neutron halo nuclei the finite-range transition amplitude has not been evaluated exactly. Additional simplifying approximations have been used—e.g., the approximation of a zero-range interaction between the core and valence neutron(s) [28,33–35]. The zero-range approximation (ZRA) implies that the projectile's internal orbital angular momentum is zero. Moreover, the ZRA cannot be justified at higher energies [31,36] even for s-wave projectiles. Several calculations of the Coulomb breakup of neutron halo nuclei have been reported [29,32,37] where finite-range effects are treated approximately by a local momentum approximation to the DWBA theory. In most of the cases studied this approach gave results which are similar to those obtained within the adiabatic model. However, in order to draw conclusions from such a comparison, regarding the basic assumptions made in the two theories, the effects of the additional approximation to the DWBA breakup amplitude must be known. Recently, test calculations within the exact DWBA theory have been presented [38]. The DWBA breakup amplitude has been expressed in momentum space as a three-dimensional integral and evaluated without the use of additional approximations. It has been shown that commonly used approximations to the DWBA theory of Coulomb breakup are very suspect.

In this paper, the method of evaluation of the DWBA breakup amplitude in momentum space is presented in more detail. The theory is applied to the Coulomb breakup of the one-neutron halo nuclei ^{11}Be and ^{19}C at energies around 70 MeV/nucleon. The calculations for relative energy spectra are compared to the experimental data of Nakamura *et al.* [10,11]. The results are also compared to the predictions of the adiabatic model as well as to those obtained using the local momentum approximation to the DWBA.
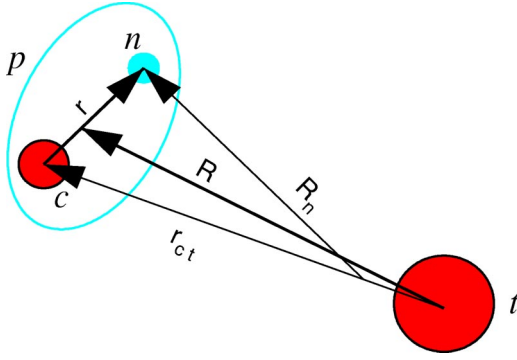
___
*Electronic address: zadro@irb.hr

FIG. 1. (Color online) Definition of the relative coordinates used in the text.

The paper is organized in the following way. In Sec. II the theoretical formalism is given. Numerical results and comparison to experimental data are presented and discussed in Sec. III. Conclusion are summarized in Sec. IV.

II. FORMALISM

We consider the reaction $p+t \rightarrow c+n+t$, where the two-body projectile p (with charge Z_p), consisting of the charged fragment c (with mass m_c and charge $Z_c=Z_p$) and the neutral particle n (with mass m_n), breaks up in the Coulomb field of a target t (with mass m_t and charge Z_t). The relative coordinates used to describe this three-body $c+n+t$ system are shown in Fig. 1. The two complementary sets of relative coordinates (r,R) and (r_{ct},R_n) are related by the following equations:

$$r_{ct} = R - \alpha r, \quad R_n = \beta R + \gamma r, \quad (1)$$

where

$$\alpha = \frac{m_n}{m_c + m_n}, \quad \beta = \frac{m_t}{m_c + m_t}, \quad \gamma = 1 - \alpha\beta. \quad (2)$$

The corresponding pairs of the relative momenta in the final channel $(\hbar k, \hbar K_f)$ and $(\hbar k_{ct}, \hbar K_n)$ are related as

$$k_{ct} = \gamma K_f - \beta k, \quad K_n = \alpha K_f + k. \quad (3)$$

The relative momentum of the projectile with respect to the target is $\hbar K_i$.

We assume that the projectile interacts with the target only through the core-target point Coulomb potential $V_{ct}(r_{ct})$. The exact transition amplitude in the post-form is given by (spin coordinates are omitted for simplicity)

$$T = \langle \chi^{(-)}(k_{ct}, r_{ct}) \Phi_c e^{iK_n \cdot R_n} \Phi_n | V_{nc}(r) | \Psi_p^{(+)}(r, R) \rangle. \quad (4)$$

Here $\Psi_p^{(+)}(r,R)$ is the full solution of the three-body scattering problem, $\chi^{(-)}(k_{ct}, r_{ct})$ is the Coulomb distorted-wave function describing the $c-t$ relative motion in the final state, and $V_{nc}(r)$ is the core-valence particle binding potential. Φ_c and Φ_n are, respectively, the internal wave functions of the fragments c and n.

A. DWBA transition amplitude

The DWBA consists of replacing the exact wave function $\Psi_p^{(+)}(r,R)$ by

$$\Psi_p^{(+)}(r,R) \approx \Phi_p(r)\chi^{(+)}(K_i,R), \quad (5)$$

where $\Phi_p(r)$ is the projectile internal wave function and $\chi^{(+)}(K_i,R)$ is the Coulomb distorted wave describing the projectile-target relative motion. Inserting Eq. (5) into Eq. (4) and integrating over internal coordinates yields (e.g., [32,38])

$$T = \sum_{\ell m j \mu} S_{\ell j}^{1/2} \langle J_c M_c j \mu | J_p M_p \rangle \langle \ell m S \sigma | j \mu \rangle B_{\ell m}, \quad (6)$$

where $S_{\ell j}^{1/2}$ is the usual spectroscopic amplitude. Here, J_c, S, and J_p are the spins of the particles c, n, and p, respectively, ℓ is the orbital angular momentum of the particle n in the projectile p, and j is its total angular momentum. The reduced transition amplitude $B_{\ell m}$ is

$$B_{\ell m} = \langle \chi^{(-)}(k_{ct}, r_{ct}) e^{iK_n \cdot R_n} | V_{nc}(r) | \phi_p^{\ell m}(r) \chi^{(+)}(K_i, R) \rangle, \quad (7)$$

where $\phi_p^{\ell m}(r)$ is the wave function of the $n-c$ relative motion in the projectile p,

$$\phi_p^{\ell m}(r) = i^\ell u_\ell(r) Y_{\ell m}(\hat{r}). \quad (8)$$

B. Approximations to the DWBA amplitude

The expression for the transition amplitude $B_{\ell m}$ is quite difficult to evaluate because it involves a six-dimensional integral. Therefore, different additional approximations have been used to reduce the computational complexity. The common result of several approximate methods [38] is that the reduced transition amplitude separates into two factors, each involving a three-dimensional integral,

$$B_{\ell m} \approx \langle e^{iq_{nc} \cdot r} | V_{nc}(r) | \phi_p^{\ell m}(r) \rangle \langle \chi^{(-)}(k_{ct}, r') e^{i\beta K_n \cdot r'} | \chi^{(+)}(K_i, r') \rangle. \quad (9)$$

The first factor in this equation is the so-called vertex function and it contains information about the internal structure of the projectile. It can be expressed as

$$F(q_{nc}) = \langle e^{iq_{nc} \cdot r} | V_{nc}(r) | \phi_p^{\ell m}(r) \rangle = F_\ell(q_{nc}) Y_{\ell m}(\hat{q}_{nc}), \quad (10)$$

where

$$F_\ell(q_{nc}) = 4\pi \int dr r^2 j_\ell(q_{nc} r) V_{nc}(r) u_\ell(r). \quad (11)$$

The amplitudes of different approaches differ only through the momenta q_{nc} which appear in the vertex function $F(q_{nc})$. The ZRA, defined by $V_{nc}(r)\phi_p^{\ell m}(r)=D_0\delta(r)$, corresponds to the constant vertex function $F(q_{nc})=D_0=F(0)$. An approximate way of taking into account finite-range effects is by use of the local momentum approximation. Applying this approximation to the entrance-channel Coulomb distorted wave $\chi^{(+)}(K_i,R)$ leads to Eq. (9) with $q_{nc}=k-\alpha(K_i'-K_f)$, where K_i' is the local momentum evaluated at some representative projectile-target distance. With the local momentum approxi-

mation to the Coulomb distorted wave in the final channel, $\chi^{(-)}(\mathbf{k}_{ct},\mathbf{r}_{ct})$, one obtains $\mathbf{q}_{nc}=\mathbf{k}-\alpha(\mathbf{k}'_{ct}-\mathbf{k}_{ct})$, where $\mathbf{k}'_{ct}$ is the effective local momentum in the core-target system. If the local momenta $\mathbf{K}'_i$ and $\mathbf{k}'_{ct}$ are replaced by their asymptotic values $\mathbf{K}_i$ and $\mathbf{k}_{ct}$ (asymptotic momentum approximation), we have $\mathbf{q}_{nc}=\mathbf{k}-\alpha(\mathbf{K}_i-\mathbf{K}_f)$ and $\mathbf{q}_{nc}=\mathbf{k}$, respectively. A detailed discussion of the validity of the approximate DWBA methods can be found in Ref. [38].

The second term in Eq. (9) contains the dynamics of the breakup process. It can be expressed in closed form in terms of hypergeometric functions—e.g., Refs. [39,40]. Using the following expressions for Coulomb distorted waves,

$$\chi^{(+)}(\mathbf{k}_{ij},\mathbf{r}_{ij}) = e^{-\pi\eta_{ij}/2}\Gamma(1+i\eta_{ij})e^{i\mathbf{k}_{ij}\cdot\mathbf{r}_{ij}}$$
$$\times {}_1F_1[-i\eta_{ij},1;i(k_{ij}r_{ij}-\mathbf{k}_{ij}\cdot\mathbf{r}_{ij})], \quad (12)$$

$$\chi^{(-)*}(\mathbf{k}_{ij},\mathbf{r}_{ij}) = \chi^{(+)}(-\mathbf{k}_{ij},\mathbf{r}_{ij}), \quad (13)$$

one obtains

$$\langle\chi^{(-)}(\mathbf{k}_{ct},\mathbf{r}')e^{i\beta\mathbf{K}_n\cdot\mathbf{r}'}|\chi^{(+)}(\mathbf{K}_i,\mathbf{r}')\rangle$$
$$= e^{-\pi(\eta_{pt}+\eta_{ct})/2}\Gamma(1+i\eta_{pt})$$
$$\times\Gamma(1+i\eta_{ct})\left[-\lim_{\varepsilon\to0}\frac{d}{d\varepsilon}I_B(\varepsilon,\mathbf{K}_i,\mathbf{k}_{ct},\mathbf{Q})\right]. \quad (14)$$

Here I_B is the integral which appears in the calculation of the bremsstrahlung cross section [41–43], sometimes called the Nordsieck integral [44],

$$I_B(\varepsilon,\mathbf{K}_i,\mathbf{k}_{ct},\mathbf{Q})$$
$$= \int\frac{d\mathbf{r}'}{r'}e^{-\varepsilon r'+i\mathbf{Q}\cdot\mathbf{r}'}{}_1F_1[-i\eta_{ct},1;i(k_{ct}r'+\mathbf{k}_{ct}\cdot\mathbf{r}')]$$
$$\times{}_1F_1[-i\eta_{pt},1;i(K_ir'-\mathbf{K}_i\cdot\mathbf{r}')]$$
$$= A(\varepsilon,\mathbf{K}_i,\mathbf{k}_{ct},\mathbf{Q})\,{}_2F_1[-i\eta_{pt},-i\eta_{ct};1;z(\varepsilon,\mathbf{K}_i,\mathbf{k}_{ct},\mathbf{Q})],$$
$$(15)$$

where

$$A(\varepsilon,\mathbf{K}_i,\mathbf{k}_{ct},\mathbf{Q}) = 4\pi\frac{(Q^2+\varepsilon^2-2\mathbf{Q}\cdot\mathbf{K}_i-2i\varepsilon K_i)^{i\eta_{pt}}(Q^2+\varepsilon^2+2\mathbf{Q}\cdot\mathbf{k}_{ct}-2i\varepsilon k_{ct})^{i\eta_{ct}}}{(Q^2+\varepsilon^2)^{1+i\eta_{pt}+i\eta_{ct}}}, \quad (16)$$

$$z(\varepsilon,\mathbf{K}_i,\mathbf{k}_{ct},\mathbf{Q}) = \frac{2(Q^2+\varepsilon^2)(K_ik_{ct}+\mathbf{K}_i\cdot\mathbf{k}_{ct})-4(\mathbf{Q}\cdot\mathbf{K}_i+i\varepsilon K_i)(\mathbf{Q}\cdot\mathbf{k}_{ct}-i\varepsilon k_{ct})}{(Q^2+\varepsilon^2-2\mathbf{Q}\cdot\mathbf{K}_i-2i\varepsilon K_i)(Q^2+\varepsilon^2+2\mathbf{Q}\cdot\mathbf{k}_{ct}-2i\varepsilon k_{ct})}, \quad (17)$$

with

$$\mathbf{Q} = \mathbf{K}_i-\mathbf{k}_{ct}-\beta\mathbf{K}_n = \mathbf{K}_i-\mathbf{K}_f. \quad (18)$$

In the above expressions ε is a real positive parameter and η_{pt} and η_{ct} are the Coulomb parameters,

$$\eta_{pt} = \frac{Z_pZ_te^2\mu_{pt}}{\hbar^2K_i}, \qquad \eta_{ct} = \frac{Z_cZ_te^2\mu_{ct}}{\hbar^2k_{ct}}, \quad (19)$$

where μ_{pt} and μ_{ct} are the reduced masses of the projectile-target and core-target systems, respectively.

C. Evaluation of the exact DWBA amplitude

The reduced amplitude of Eq. (7) can be expressed in momentum space as a three-dimensional integral,

$$B_{\ell m} = \int\frac{d\mathbf{Q}_i}{(2\pi)^3}F[\mathbf{k}-\alpha(\mathbf{Q}_i-\mathbf{K}_f)]\widetilde{\chi}^{(-)*}(\mathbf{k}_{ct},\mathbf{Q}_i-\mathbf{K}_f+\mathbf{k}_{ct})$$
$$\times\widetilde{\chi}^{(+)}(\mathbf{K}_i,\mathbf{Q}_i), \quad (20)$$

where $F(\mathbf{q}),\mathbf{q}=\mathbf{k}-\alpha(\mathbf{Q}_i-\mathbf{K}_f)$, is the vertex function defined by Eq. (10) and $\widetilde{\chi}^{(\pm)}(\mathbf{k}_{ij},\mathbf{q}_{ij})$ is the Fourier transform of the Coulomb wave function $\chi^{(\pm)}(\mathbf{k}_{ij},\mathbf{r}_{ij})$ defined by

$$\chi^{(+)}(\mathbf{k}_{ij},\mathbf{r}_{ij}) = \int\frac{d\mathbf{q}_{ij}}{(2\pi)^3}e^{i\mathbf{q}_{ij}\cdot\mathbf{r}_{ij}}\widetilde{\chi}^{(+)}(\mathbf{k}_{ij},\mathbf{q}_{ij}), \quad (21)$$

$$\widetilde{\chi}^{(+)}(\mathbf{k}_{ij},\mathbf{q}_{ij}) = \int d\mathbf{r}_{ij}e^{-i\mathbf{q}_{ij}\cdot\mathbf{r}_{ij}}\chi^{(+)}(\mathbf{k}_{ij},\mathbf{r}_{ij}). \quad (22)$$

The Coulomb wave in momentum space has been derived by Guth and Mullin [45]. It can be can be expressed as

$$\widetilde{\chi}^{(+)}(\mathbf{k}_{ij},\mathbf{q}_{ij}) = \varphi_0^{(+)}(\mathbf{k}_{ij},\mathbf{q}_{ij}) + \varphi^{(+)}(\mathbf{k}_{ij},\mathbf{q}_{ij}), \quad (23)$$

where

$$\varphi^{(+)}(\mathbf{k}_{ij},\mathbf{q}_{ij}) = -8\pi\eta_{ij}k_{ij}e^{-\pi\eta_{ij}/2}\Gamma(1+i\eta_{ij})$$
$$\times\lim_{\varepsilon\to0}\left\{\frac{[q_{ij}^2-(k_{ij}+i\varepsilon)^2]^{-1+i\eta_{ij}}}{[|\mathbf{q}_{ij}-\mathbf{k}_{ij}|^2+\varepsilon^2]^{1+i\eta_{ij}}}\right\}. \quad (24)$$

The first term in Eq. (23) is the Coulomb asymptotic state in momentum representation [46]. It is a δ-function-type term with support at the point $\mathbf{q}_{ij}=\mathbf{k}_{ij}$.

Now, we assume that the dominant contribution to the integral in Eq. (20) comes from the narrow region around a point $\mathbf{Q}_i=\mathbf{Q}_i^0$ and that $F(\mathbf{q})$ is the slowly varying function of $\mathbf{Q}_i$, so that it can be factored out of the integral at the point $\mathbf{q}_{nc}=\mathbf{k}-\alpha(\mathbf{Q}_i^0-\mathbf{K}_f)$. Then the breakup amplitude reduces to

$$B_{\ell m} \approx B_{\ell m}^0 = F[k - \alpha(Q_i^0 - K_f)] \int \frac{dQ_i}{(2\pi)^3}$$
$$\times \widetilde{\chi}^{(-)*}(k_{ct}, Q_i - K_f + k_{ct}) \widetilde{\chi}^{(+)}(K_i, Q_i)$$
$$= F(q_{nc}) \langle \chi^{(-)}(k_{ct}, R) e^{i\beta K_n \cdot R} | \chi^{(+)}(K_i, R) \rangle. \quad (25)$$

This expression for $B_{\ell m}$ has the same structure as that in Eq. (9). The localization of the breakup amplitude (20) in momentum q and the validity of the factorization approximation for different choices of the effective momentum Q_i^0 has been studied in Ref. [38].

The exact transition amplitude can be rewritten as

$$B_{\ell m} = B_{\ell m}^0 + \Delta B_{\ell m}, \quad (26)$$

where

$$\Delta B_{\ell m} = \int \frac{dQ_i}{(2\pi)^3} \{ F[k - \alpha(Q_i - K_f)] - F[k - \alpha(Q_i^0 - K_f)] \}$$
$$\times \widetilde{\chi}^{(-)*}(k_{ct}, Q_i - K_f + k_{ct}) \widetilde{\chi}^{(+)}(K_i, Q_i). \quad (27)$$

In order to reduce the integral in Eq. (27), we write it as

$$\Delta B_{\ell m} = \Delta B_{\ell m}^0 + \delta B_{\ell m}, \quad (28)$$

where

$$\Delta B_{\ell m}^0 = \int \frac{dQ_i}{(2\pi)^3} f^0(Q_i) \widetilde{\chi}^{(-)*}(k_{ct}, Q_i - K_f + k_{ct}) \widetilde{\chi}^{(+)}(K_i, Q_i), \quad (29)$$

$$\delta B_{\ell m} = \int \frac{dQ_i}{(2\pi)^3} [f(Q_i) - f^0(Q_i)] \widetilde{\chi}^{(-)*}(k_{ct}, Q_i - K_f + k_{ct})$$
$$\times \widetilde{\chi}^{(+)}(K_i, Q_i), \quad (30)$$

with

$$f(Q_i) = F[k - \alpha(Q_i - K_f)] - F[k - \alpha(Q_i^0 - K_f)], \quad (31)$$

$$f^0(Q_i) = \frac{Q_i^2 - K_i^2}{K_f^2 - K_i^2} f(K_f) + \frac{(Q_i - K_f + k_{ct})^2 - k_{ct}^2}{(K_i - K_f + k_{ct})^2 - k_{ct}^2} f(K_i). \quad (32)$$

It is readily seen that $[f(Q_i) - f^0(Q_i)] \rightarrow 0$ when $Q_i \rightarrow K_i$ and $Q_i \rightarrow K_f$, which are the supports of $\varphi_0^{(+)}(K_i, Q_i)$ and $\varphi_0^{(-)*}(k_{ct}, Q_i - K_f + k_{ct})$, respectively. Thus, the contribution from terms involving the Coulomb asymptotic states in Eq. (30) vanishes, so that we can write

$$\delta B_{\ell m} = \int \frac{dQ_i}{(2\pi)^3} [f(Q_i) - f^0(Q_i)] \varphi^{(-)*}(k_{ct}, Q_i - K_f + k_{ct})$$
$$\times \varphi^{(+)}(K_i, Q_i). \quad (33)$$

The first term in Eq. (28) can be evaluated analytically. Using the Schrödinger equation in momentum space, one obtains

$$(q_{ij}^2 - k_{ij}^2) \widetilde{\chi}^{(+)}(k_{ij}, q_{ij}) = -2\eta_{ij} k_{ij} \widetilde{W}^{(+)}(k_{ij}, q_{ij}), \quad (34)$$

where $\widetilde{W}^{(+)}(k_{ij}, q_{ij})$ is the Fourier transform of $\chi^{(+)}(k_{ij}, r_{ij})/r_{ij}$, and the term $\Delta B_{\ell m}^0$ can be written as

$$\Delta B_{\ell m}^0 = -\frac{2\eta_{pt} K_i f(K_f)}{K_f^2 - K_i^2} \int \frac{dQ_i}{(2\pi)^3} \widetilde{\chi}^{(-)*}(k_{ct}, Q_i - K_f + k_{ct})$$
$$\times \widetilde{W}^{(+)}(K_i, Q_i) - \frac{2\eta_{ct} k_{ct} f(K_i)}{(Q_i - K_f + k_{ct})^2 - k_{ct}^2} \int \frac{dQ_i}{(2\pi)^3}$$
$$\times \widetilde{W}^{(-)*}(k_{ct}, Q_i - K_f + k_{ct}) \widetilde{\chi}^{(+)}(K_i, Q_i). \quad (35)$$

Transforming these integrals back to coordinate space, we find

$$\Delta B_{\ell m}^0 = -2 \left[\frac{\eta_{pt} K_i f(K_f)}{K_f^2 - K_i^2} + \frac{\eta_{ct} k_{ct} f(K_i)}{(Q_i - K_f + k_{ct})^2 - k_{ct}^2} \right]$$
$$\times \left\langle \chi^{(-)}(k_{ct}, R) e^{i(K_f - k_{ct}) \cdot R} \left| \frac{1}{R} \right| \chi^{(+)}(K_i, R) \right\rangle$$
$$= -2 \left[\frac{\eta_{pt} K_i f(K_f)}{K_f^2 - K_i^2} + \frac{\eta_{ct} k_{ct} f(K_i)}{(Q_i - K_f + k_{ct})^2 - k_{ct}^2} \right]$$
$$\times e^{-\pi(\eta_{pt} + \eta_{ct})/2} \Gamma(1 + i\eta_{pt}) \Gamma(1 + i\eta_{ct})$$
$$\times \lim_{\varepsilon \to 0} I_B(\varepsilon, K_i, k_{ct}, Q), \quad (36)$$

where I_B is the Nordsieck integral given by Eq. (15) with $Q = K_i - k_{ct} - (K_f - k_{ct}) = K_i - K_f$.

Thus, the DWBA breakup amplitude of Eq. (20) can be reexpressed as

$$B_{\ell m} = B_{\ell m}^0 + \Delta B_{\ell m}^0 + \delta B_{\ell m}. \quad (37)$$

The terms $B_{\ell m}^0$ and $\Delta B_{\ell m}^0$ have the analytical forms of Eq. (25) and Eq. (36), respectively. The integration in the expression (33) for $\delta B_{\ell m}$ can be carried out numerically.

D. Adiabatic model

The Coulomb breakup of neutron halo nuclei has recently been formulated within the adiabatic model [30–32]. In the adiabatic approach it is assumed that the projectile excitation energy is negligible compared to the incident energy, and thus the internal Hamiltonian of the projectile can be replaced by a representative constant energy. This is chosen to be the $n-c$ binding energy in the projectile ground state. It has been shown that the resulting three-body wave function has an analytic solution [47]

$$\Psi_p^{(+)}(r, R) \approx \Psi_p^{(+)AD}(r, R) = \Phi_p(r) e^{i\alpha K_i \cdot r} \chi^{(+)}(K_i, R). \quad (38)$$

Substituting $\Psi_p^{(+)AD}$ in Eq. (4) leads to the expression (6) for the transition amplitude where the reduced amplitude $B_{\ell m}$ is

$$B_{\ell m}^{AD} = \langle e^{iq_{nc} \cdot r} | V_{nc}(r) | \phi_p^{\ell m}(r) \rangle \langle \chi^{(-)}(k_{ct}, r_{ct}) e^{i\beta K_n \cdot r_{ct}} | \chi^{(+)}(K_i, r_{ct}) \rangle, \quad (39)$$

with $q_{nc} = k - \alpha(K_i - K_f)$. It may be noted that the identical amplitude is obtained within the DWBA theory by making the asymptotic momentum approximation to the entrance-

channel Coulomb distorted wave. However, assumptions underlying the two theories are quite different [32].

E. Differential cross section

The differential cross section for the three-body breakup reaction is given by (e.g., [48,49])

$$d\sigma = \frac{2\pi\mu_{pt}}{\hbar p_{pt}} \frac{1}{2J_p+1} \sum_{M_c\sigma M_p} |T|^2 \frac{d\boldsymbol{p}_{nc}d\boldsymbol{p}_{(nc)t}}{(2\pi\hbar)^6}$$

$$\times \delta(E_{nc} + E_{(nc)t} - E_{tot}^{c.m.}), \quad (40)$$

where $p_{pt}=\hbar K_i$, $\boldsymbol{p}_{nc}=\hbar k$, and $\boldsymbol{p}_{(nc)t}=\hbar K_f$. In Eq. (40), E_{nc} and $E_{(nc)t}$ are the kinetic energies of the relative motion of the fragments n and c and of their center of mass (c.m.) with respect to the target, respectively. The total kinetic energy in the c.m. system, $E_{tot}^{c.m.}$, is related to the kinetic energy of the projectile-target relative motion E_{pt} and the reaction Q value Q,

$$E_{tot}^{c.m.} = E_{nc} + E_{(nc)t} = E_{pt} + Q. \quad (41)$$

Using $p_{ij}dp_{ij}=\mu_{ij}dE_{ij}$, where μ_{ij} is the corresponding reduced mass, one obtains, for the triple differential cross section,

$$\frac{d^3\sigma}{dE_{nc}d\Omega_{nc}d\Omega_{(nc)t}} = \frac{2\pi\mu_{pt}}{\hbar p_{pt}} \frac{1}{2J_p+1} \sum_{M_c\sigma M_p} |T|^2 \rho_f, \quad (42)$$

Here Ω_{nc} and $\Omega_{(nc)t}$ are the solid angles associated with the directions of the relative momenta $\boldsymbol{p}_{nc}$ and $\boldsymbol{p}_{(nc)t}$, respectively, and ρ_f is the phase space factor,

$$\rho_f = \frac{\mu_{nc}\mu_{(nc)t}p_{nc}p_{(nc)t}}{(2\pi\hbar)^6}. \quad (43)$$

Inserting Eq. (6) into Eq. (42) and carrying out the sum over spin projections one gets

$$\frac{d^3\sigma}{dE_{nc}d\Omega_{nc}d\Omega_{(nc)t}} = \frac{2\pi\mu_{pt}}{\hbar p_{pt}} \sum_{j\ell m} \frac{S_{\ell j}}{(2\ell+1)} |B_{\ell m}|^2 \rho_f. \quad (44)$$

Finally, the relative energy spectrum $d\sigma/dE_{nc}$ is obtained bay integrating this equation over the solid angles Ω_{nc} and $\Omega_{(nc)t}$.

III. NUMERICAL RESULTS

The breakup of the ^{11}Be and ^{19}C halo nuclei on a Pb target has been measured at RIKEN at the beam energies of 72 and 67 MeV/nucleon, respectively [10,11]. In this section the calculations within the exact DWBA model are presented for these cases. For the purpose of comparison with the DWBA results, calculations were also performed within the adiabatic (AD) model. Comparison is also made with the results obtained by using the local momentum approximation to the DWBA (LMA-DWBA). The local momentum approximation was applied to the distorted wave in the final channel. The local momentum $\boldsymbol{k}'_{ct}$ was calculated as in Refs. [29,37]: the magnitude of $\boldsymbol{k}'_{ct}$ was evaluated at 10 fm and its direction

TABLE I. Parameters of the n-^{10}Be and n-^{18}C potentials.

Nucleus	a [fm]	R [fm]	Set	Ref.
^{11}Be	0.50	2.478	P1	[32]
	0.60	2.669	P2	[50]
	0.67	2.640	P3	[51]
^{19}C	0.62	3.239		[11]

was taken to be the same as that of the asymptotic momentum $\boldsymbol{k}_{ct}$.

The single-particle wave functions $u_\ell(r)$ were calculated in a Woods-Saxon potential. The depth of the potential was adjusted to reproduce the neutron-core separation energy. The radius and diffuseness parameters used in this work are listed in Table I. For ^{11}Be, the ground state was assumed to have a $2s_{1/2}$ neutron coupled to the ^{10}Be(0^+) core with a binding energy of 504 keV. In the case of ^{19}C, the ground-state wave function was obtained by assuming a configuration in which a $2s_{1/2}$ neutron is bound by 0.530 keV to the ^{18}C(0^+) core [11].

The cross section $d\sigma/dE_{\text{rel}}$ as a function of the relative energy E_{rel} ($E_{\text{rel}}=E_{nc}$) between the fragments n and ^{10}Be from the breakup of ^{11}Be on a ^{208}Pb target at the beam energy of 72 MeV/nucleon is shown in Fig. 2. The relative energy spectrum is obtained by integrating the triple-
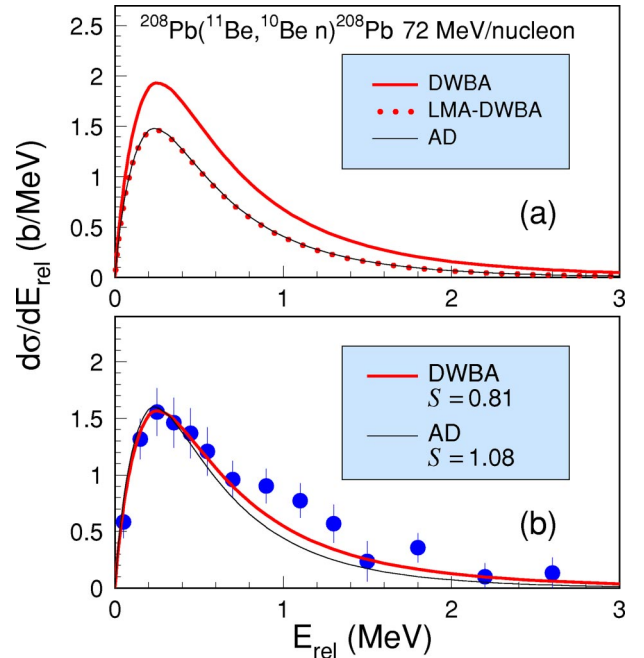

FIG. 2. (Color online) (a) Cross section as a function of the relative energy between the neutron and ^{10}Be emitted in the breakup of ^{11}Be on ^{208}Pb at the beam energy of 72 MeV/nucleon. The curves represent the exact DWBA (thick solid), the LMA-DWBA (dotted), and the AD model (thin solid) calculations. The calculations are with the potential set $P2$ of Table I. (b) The exact DWBA and AD model calculations after multiplying with a spectroscopic factor of 0.81 and 1.08, respectively. The experimental data are from Ref. [10], but scaled by a factor 0.85 [9].
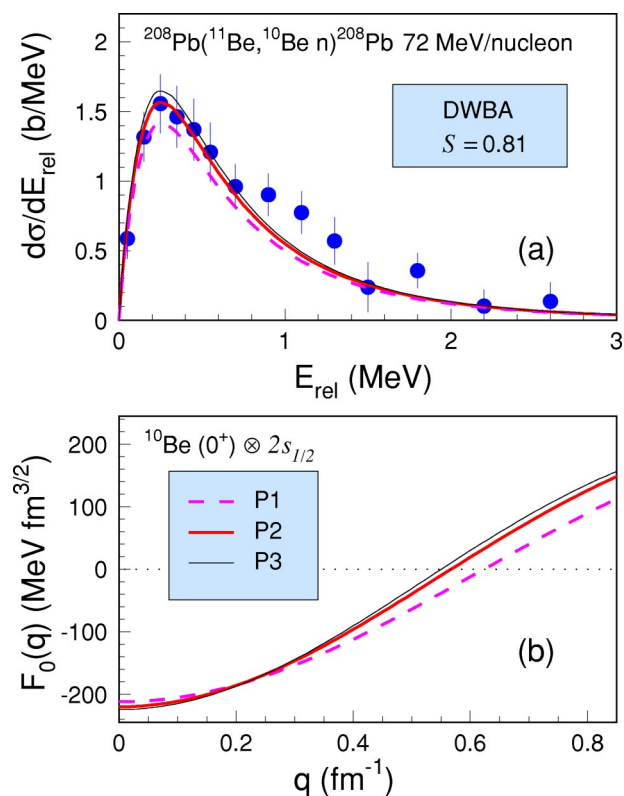
FIG. 3. (Color online) (a) Cross section as a function of the n-^{10}Be relative energy for the breakup of ^{11}Be on ^{208}Pb at the beam energy of 72 MeV/nucleon. The experimental data are from Ref. [10], but scaled by a factor 0.85 [9]. The curves compare the exact DWBA calculations for three different shapes of the n-^{10}Be potential (see Table I): P1 (thick solid), P2 (dashed), and P3 (thin solid). (b) The vertex functions $F_0(q)$, as a function of q, for these potentials.

FIG. 4. (Color online) (a) Cross section as a function of the n-^{18}C relative energy for the breakup of ^{19}C on ^{208}Pb at the beam energy of 67 MeV/nucleon. The curves represent the exact DWBA (thick solid), the LMA-DWBA (dotted), and the AD model (thin solid) calculations. The calculations are for the neutron separation energy of 530 keV. (b) The exact DWBA and AD model calculations after multiplying with a spectroscopic factor of 0.73 and 1.08, respectively. The experimental data are from Ref. [11].

differential cross section $d^3\sigma/dE_{nc}d\Omega_{nc}d\Omega_{(nc)t}$, Eq. (44), over all possible relative angles between the fragments. The integration over c.m. angles of the $n+^{10}$Be system $\theta_{(nc)t}$ was done in the range $0°$–$2.77°$, which corresponds to a minimum impact parameter b_{min} of about 13 fm. The thick solid and dotted lines represent the results of the exact DWBA and LMA-DWBA calculations, respectively. The results of the AD model are represented by the thin solid line. It can be seen in Fig. 2(a) that the results of the exact DWBA differ considerably from the results of the approximate DWBA as well as from those of the AD model. On the other hand, the results of the LMA-DWBA are almost identical to the results of the AD model. The comparison of the results of the exact DWBA and AD model calculations with the experimental data of Nakamura *et al.* [10] is presented in Fig. 2(b). The experimental data are scaled by a factor of 0.85 (see Ref. [9]) and the theoretical cross sections are multiplied by a spectroscopic factor of 0.81 (DWBA) and 1.08 (AD). These values of the spectroscopic factor S are deduced by fitting the calculated cross sections to the experimental spectrum for low relative energies, $E_{rel} < 0.8$ MeV.

The calculated cross section depends on the parameters defining the geometry of the Woods-Saxon potential. Changing the shape of the binding potential will change the size of
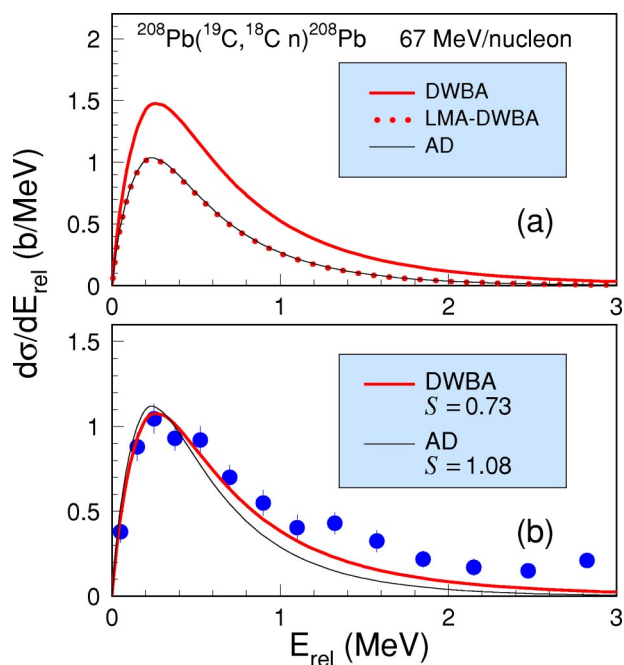
the neutron halo. The exact DWBA calculations for three sets of the radius parameter R and diffuseness a (see Table I) are presented in Fig. 3(a). The corresponding root-mean-square (rms) radii for the relative motion between the halo neutron and the core are 6.7 fm (P1), 7.0 fm (P2), and 7.15 fm (P3). The resulting spectroscopic factors are 0.90, 0.81, and 0.77, respectively. The rms radius is sensitive to the potential diffuseness while its dependence on the potential radius is rather weak [51]. The structure of the projectile enters through the vertex function $F_0(q)$. Figure 3(b) shows the low-momentum part of the vertex functions for ^{11}Be, as a function of q, for the three potentials. The breakup cross sections at very forward angles reflect the behavior of the vertex function at low momenta q; see Ref. [38].

Figure 4 shows the cross sections as a function of the relative energy between the fragments (neutron and ^{18}C) for the breakup of ^{19}C on a ^{208}Pb target at the beam energy of 67 MeV/nucleon. The integration over $\theta_{(nc)t}$ was done in the range $0°$–$2.5°$ [52]. The calculations are for the neutron separation energy $S_n = 530$ keV [11]. Qualitatively, the results of the three models for the ^{19}C breakup are similar to those for the ^{11}Be case. The spectroscopic factor $S = 0.73$ is obtained by fitting the exact DWBA results to the experimental data for $E_{rel} < 1$ MeV. The results of the AD model differ significantly from the exact DWBA calculations: they lead to a spectroscopic factor of 1.08. We note that in this case too the effects of the local momentum approximation to the DWBA breakup amplitude are significant.
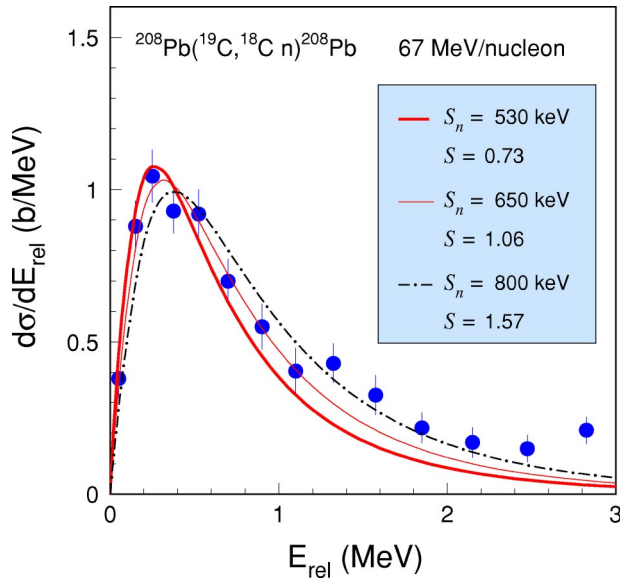
FIG. 5. (Color online) Cross section as a function of the n-^{18}C relative energy for the breakup of ^{19}C on ^{208}Pb at the beam energy of 67 MeV/nucleon. The curves represent the exact DWBA calculations for three values of the neutron-core separation energy S_n: 530 keV (thick solid), 650 keV (thin solid), and 800 keV (dot-dashed). The experimental data are from Ref. [11].

Since the one-neutron separation energy S_n of the ^{19}C is not known precisely, calculations were performed with three values of S_n: 530 keV [11], 650 keV [5,53], and 800 keV [53]. The results of the exact DWBA calculations are shown in Fig. 5. It can be noted that both the peak height and shape of the relative energy spectrum are quite sensitive to the separation energy. The normalization factor S changes from 0.73 for S_n=530 keV to 1.57 for S_n=800 keV. The comparison of the shapes of the calculations and experimental data in the peak region seems to support a value of S_n in the range ~530–650 keV.

In order to draw more reliable conclusions from a comparison of the pure Coulomb breakup calculations with experimental data, the effects of the projectile-target nuclear interaction should be known. In the present calculations the nuclear absorption is simulated by a cutoff on the angle $\theta_{(nc)t}$. This classically corresponds to a cutoff on the impact parameters b. However, the choice of an adequate minimum impact parameter b_{min} is not straightforward for halo nuclei. Furthermore, one has to take into account the nuclear contribution to the breakup cross section. In Refs. [10,11], this was estimated from the carbon target data. Recently, a different approach has been used [12–14]: the breakup cross sections for ^{11}Be, ^{15}C, and ^{19}C have been analyzed as a function of the minimum impact parameter. The selection of the minimum impact parameter is expected to be effective to select the pure Coulomb breakup component. In order to make a comparison with the new RIKEN data (preliminary experimental data of Refs. [12–14], the DWBA and AD model calculations were performed with the minimum impact parameter b_{min} =30 fm. The results for the breakup of ^{11}Be at 68 MeV/nucleon and ^{19}C at 67 MeV/nucleon on ^{208}Pb are shown in Fig. 6. For ^{11}Be, the calculations and new data for
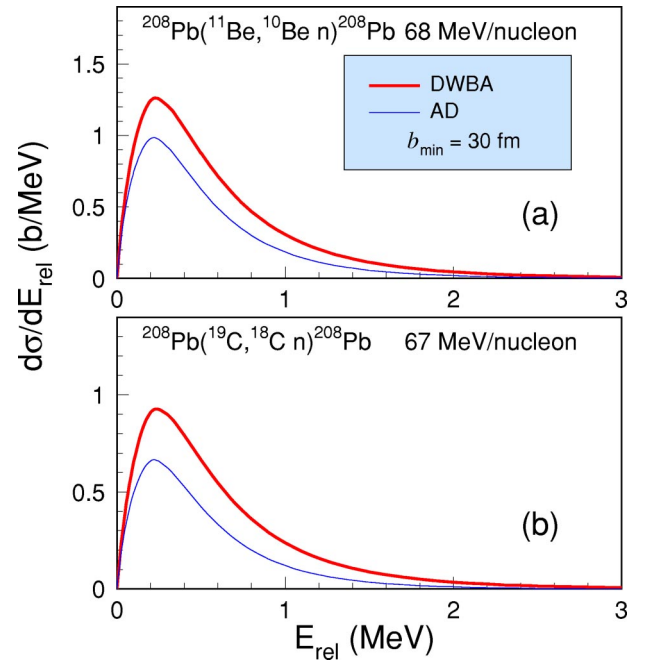
FIG. 6. (Color online) Cross section as a function of the neutron-core relative energy for the breakup of (a) ^{11}Be on ^{208}Pb at the beam energy of 68 MeV/nucleon and (b) ^{19}C on ^{208}Pb at the beam energy of 67 MeV/nucleon, for a minimum impact parameter of b_{min}=30 fm. The curves represent the exact DWBA (thick line) and the AD model (thin line) calculations. The calculations for the ^{11}Be projectile are with the potential set P2 of Table I. The calculations for ^{19}C are with the neutron-core separation energy S_n =530 keV.

$b>30$ fm [12–14] seem to lead to a spectroscopic factor smaller than that extracted from the comparison of the old data, without the selection on the impact parameter b, with the calculations for b_{min}=13 fm. In the ^{19}C case, the calculations in Fig. 6 and the data for $b>30$ [13] seem to indicate a value of S similar to that obtained from the data without the cutoff on b and the calculations with $\theta_{(nc)t}^{max}$=2.5°. More detailed comparison has to wait for the publication of the new RIKEN data.

The experimental data [10,11] could also contain contributions from the inelastic Coulomb breakup, where the target is excited during the breakup process, as well as the Coulomb breakup leading to the core excited states. In the Coulomb breakup experiments of Refs. [15,16,54], γ rays were measured in coincidence with the breakup fragments. The detection of γ rays allowed to identify the specific states of the core after breakup. In addition, the γ rays associated with the excitation of the target were measured in the experiment of Ref. [54]. The results of these experiments suggest that the mutual excitation process could be negligible in the Coulomb breakup reactions. In Ref. [16] it was found that in the the Coulomb breakup of ^{11}Be on Pb at 520 MeV/nucleon a few percent of the total cross section is due to the population of the ^{10}Be excited states. Such contributions in the RIKEN data [10,11] would reduce the extracted spectroscopic factors for the core ground-state component in the ground state of ^{11}Be and ^{19}C.

IV. SUMMARY AND CONCLUSIONS

In this paper, the Coulomb breakup of one-neutron halo nuclei has been studied within the postform DWBA theory. The DWBA breakup amplitude has been evaluated in momentum space without the use of additional approximations.

Relative energy spectra of the fragments (neutron and core) were calculated for the Coulomb breakup of ^{11}Be and ^{19}C on a ^{208}Pb target at the beam energy of ~ 70 MeV/nucleon for very forward angles. The calculations have been compared with the experimental data of Nakamura *et al.* [10,11]. Good agreement in shape between the theory and the data is found for low relative energies for both projectiles. The comparison confirms that the dominant configuration of the ^{11}Be is a $2s_{1/2}$ neutron coupled to the ground state of the ^{10}Be core. For ^{19}C, the relative energy spectrum is consistent with a predominance of the ground-state configuration in which a $2s_{1/2}$ neutron is coupled to the ground state of the ^{18}C core with a binding energy in the range 530–650 keV.

The calculations were also performed within the approximate DWBA model which uses the local momentum approximation to the DWBA breakup amplitude. This work has shown that the differences between the local momentum and

exact DWBA calculations are substantial for both projectiles. In the case of the ^{11}Be breakup, the local momentum approximation reduces the cross sections in the peak region by $\sim 25\%$. In the ^{19}C case, the effects of the local momentum approximation are $\sim 35\%$. Thus, it appears that the LMA-DWBA breakup amplitude is a poor approximation to the exact DWBA amplitude.

The results of the exact DWBA calculations have also been compared to those of the AD breakup model. It appears that these two theories lead to significantly different spectroscopic factors. Thus, at least one of the models is not adequate for a quantitative analysis of the Coulomb breakup of ^{11}Be and ^{19}C at ~ 70 MeV/nucleon. This discrepancy between the DWBA and AD model results reflects differences between assumptions made in the two theories. The AD model assumes that excitations of the projectile are to the low-energy continuum, and so the adiabatic approximation can be made. Thus, there is a need to estimate the range of validity of the adiabatic approximation for the Coulomb breakup. The DWBA assumes that excitations of the projectile are weak and so need be treated only to first order. However, in the case of weakly bound halo nuclei, the effects of halo breakup could be important.

[1] K. Riisager, Rev. Mod. Phys. **66**, 1105 (1994).
[2] P. G. Hansen, A. S. Jensen, and B. Jonson, Annu. Rev. Nucl. Part. Sci. **45**, 591 (1995).
[3] I. Tanihata, J. Phys. G **22**, 157 (1996).
[4] G. Baur, K. Hencken, and D. Trautmann, Prog. Part. Nucl. Phys. **51**, 487 (2003).
[5] S. Typel and R. Shyam, Phys. Rev. C **64**, 024605 (2001).
[6] M. Fallot, J. A. Scarpaci, D. Lacroix, P. Chomaz, and J. Margueron, Nucl. Phys. **A700**, 70 (2002).
[7] R. Chatterjee and R. Shyam, Phys. Rev. C **66**, 061601(R) (2002).
[8] J. Margueron, A. Bonaccorso, and D. M. Brink, Nucl. Phys. **A720**, 337 (2003).
[9] P. Capel, D. Baye, and V. S. Melezhik, Phys. Rev. C **68**, 014612 (2003).
[10] T. Nakamura *et al.*, Phys. Lett. B **331**, 296 (1994).
[11] T. Nakamura *et al.*, Phys. Rev. Lett. **83**, 1112 (1999).
[12] N. Fukuda *et al.*, Prog. Theor. Phys. Suppl. **146**, 462 (2002).
[13] T. Nakamura *et al.*, Nucl. Phys. **A722**, 301c (2003).
[14] T. Nakamura, Nucl. Phys. **A734**, 319 (2004).
[15] U. Datta Pramanik *et al.*, Phys. Lett. B **551**, 63 (2003).
[16] R. Palit *et al.*, Phys. Rev. C **68**, 034318 (2003).
[17] S. Typel and G. Baur, Nucl. Phys. **A573**, 486 (1994).
[18] S. Typel and G. Baur, Phys. Rev. C **64**, 024601 (2001).
[19] L. F. Canto, R. Donangelo, A. Romanelli, and H. Schulz, Phys. Lett. B **318**, 415 (1993).
[20] C. A. Bertulani, L. F. Canto, and M. S. Hussein, Phys. Lett. B **353**, 413 (1995).
[21] T. Kido, K. Yabana, and Y. Suzuki, Phys. Rev. C **50**, R1276 (1994).
[22] G. F. Bertsch and C. A. Bertulani, Nucl. Phys. **A556**, 136 (1993).
[23] T. Kido, K. Yabana, and Y. Suzuki, Phys. Rev. C **53**, 2296 (1996).
[24] C. A. Bertulani and G. F. Bertsch, Phys. Rev. C **49**, 2839 (1994).
[25] H. Esbensen, G. F. Bertsch, and C. A. Bertulani, Nucl. Phys. **A581**, 107 (1995).
[26] V. S. Melezhik and D. Baye, Phys. Rev. C **59**, 3232 (1999).
[27] G. Baur, F. Rösel, D. Trautmann, and R. Shyam, Phys. Rep. **111**, 333 (1984).
[28] R. Shyam, P. Banerjee, and G. Baur, Nucl. Phys. **A540**, 341 (1992).
[29] R. Chatterjee, P. Banerjee, and R. Shyam, Nucl. Phys. **A675**, 477 (2000).
[30] J. A. Tostevin *et al.*, Phys. Lett. B **424**, 219 (1998).
[31] J. A. Tostevin, S. Rugmai, and R. C. Johnson, Phys. Rev. C **57**, 3225 (1998).
[32] P. Banerjee, I. J. Thompson, and J. A. Tostevin, Phys. Rev. C **58**, 1042 (1998).
[33] P. Banerjee and R. Shyam, Nucl. Phys. **A561**, 112 (1993).
[34] P. Banerjee and R. Shyam, Phys. Lett. B **318**, 268 (1993).
[35] P. Banerjee and R. Shyam, J. Phys. G **22**, L79 (1996).
[36] R. Shyam and M. A. Nagarajan, Ann. Phys. (N.Y.) **163**, 265 (1985).
[37] R. Shyam and P. Danielewicz, Phys. Rev. C **63**, 054608 (2001).
[38] M. Zadro, Phys. Rev. C **66**, 034603 (2002).
[39] L. Landau and E. Lifshitz, Zh. Eksp. Teor. Fiz. **18**, 750 (1948).
[40] G. Baur and D. Trautmann, Nucl. Phys. **A191**, 321 (1972).
[41] A. Sommerfeld, *Atombau und Spektrallinien* (Vieweg, Braunschweig, 1939), Vol. 2.

[42] L. Bess, Phys. Rev. **77**, 550 (1950).

[43] A. Nordsieck, Phys. Rev. **93**, 785 (1954).

[44] M. S. Gravielle and J. E. Miraglia, Comput. Phys. Commun. **69**, 53 (1992).

[45] E. Guth and C. J. Mullin, Phys. Rev. **83**, 667 (1951).

[46] H. van Haeringen, J. Math. Phys. **17**, 995 (1976).

[47] R. C. Johnson, J. S. Al-Khalili, and J. A. Tostevin, Phys. Rev. Lett. **79**, 2771 (1997).

[48] R. G. Newton, *Scattering Theory of Waves and Particles* (McGraw-Hill, New York, 1966).

[49] J. R. Taylor, *Scattering Theory* (Wiley, New York, 1972).

[50] P. Capel, D. Baye, and V. S. Melezhik, Phys. Lett. B **552**, 145 (2003).

[51] A. Muta and T. Otsuka, Prog. Theor. Phys. Suppl. **142**, 355 (2001).

[52] P. Banerjee and R. Shyam, Phys. Rev. C **61**, 047301 (2000).

[53] V. Maddalena *et al.*, Phys. Rev. C **63**, 024613 (2001).

[54] T. Kikuchi *et al.*, Phys. Lett. B **391**, 261 (1997).